Quantum circuits for the realization of equivalent forms of one-dimensional discrete-time quantum walks on near-term quantum hardware

Shivani Singh, C. Huerta Alderete, Radhakrishnan Balu, Christopher Monroe, Norbert M. Linke, and C. M. Chandrashekar

Phys. Rev. A **104**, 062401 — Published 1 December 2021

DOI: 10.1103/PhysRevA.104.062401

Quantum circuits for the realization of equivalent forms of one-dimensional discrete-time quantum walks on near-term quantum hardware

Shivani Singh,[1, 2] C. Huerta Alderete,[3, 4] Radhakrishnan Balu,[5, 6]
Christopher Monroe,[3] Norbert M. Linke,[3] and C. M. Chandrashekar[1, 2]

[1] *The Institute of Mathematical Sciences, C. I. T. Campus, Taramani, Chennai 600113, India*
[2] *Homi Bhabha National Institute, Training School Complex, Anushakti Nagar, Mumbai 400094, India*
[3] *Joint Quantum Institute, Department of Physics and Joint Center for Quantum Information and Computer Science, University of Maryland, College Park, MD 20742, USA*
[4] *Instituto Nacional de Astrofísica, Óptica y Electrónica, Calle Luis Enrique Erro No. 1, Sta. Ma. Tonantzintla, Pue. CP 72840, Mexico*
[5] *U.S. Army Research Laboratory, Computational and Information Sciences Directorate, Adelphi, Maryland 20783, USA*
[6] *Department of Mathematics & Norbert Wiener Center for Harmonic Analysis and Applications, University of Maryland, College Park, MD20742*

Quantum walks are a promising framework for developing quantum algorithms and quantum simulations. They represent an important test case for the application of quantum computers. Here we present different form of discrete-time quantum walks (DTQWs) and show their equivalence for physical realizations. Using an appropriate digital mapping of the position space on which a walker evolves to the multi-qubit states of a quantum processor, we present different configurations of quantum circuits for the implementation of DTQWs in one-dimensional position space. We provide example circuits for five-qubit processor and address scalability to higher dimensions as well as larger quantum processors.

I. INTRODUCTION

There is a great interest in developing quantum algorithms for potential speedups over conventional computers, and progress is being made in mapping such algorithms to current technology [1, 2]. Device architecture, qubit connectivity, gate fidelity, and qubit coherence time are metrics that define the trade-off in designing device specific circuits. Quantum walks [3, 4], exploiting quantum superposition of multiple paths, have played an important role in development of a wide variety of quantum algorithms. Examples include algorithms for quantum search [5–9], graph isomorphism problems [10–12], ranking nodes in a network [13–16], and quantum simulation at low and high energy scales [17–26].

There are two main variants of quantum walks, the discrete-time quantum walk (DTQW) [27, 28] and the continuous-time quantum walk (CTQW) [29, 30]. The DTQW is defined on a Hilbert space comprising internal states of the single particle called coin space and position space with the evolution being driven by a position shift operator controlled by a quantum coin operator. The CTQW is defined directly on the position Hilbert space with the evolution being driven by the Hamiltonian of the system and adjacency matrix of the position space. In both variants, the probability distribution of the particle spreads quadratically faster in position space compared to the classical random walk [31–35].

Due to the Hilbert space configuration of DTQWs one can define many different forms of quantum coin operators and position shift operators that controls the dynamics leading to variants such as the standard DTQW, directed DTQW [36–38], split-step DTQW [39–41], and the Szegedy walk [42]. These models have been successfully used to mimic different quantum phenomenon such as Dirac cellular automata [41, 43, 44], strong and weak localization [45, 46], topological phases [47, 48], and many more.

Experimental implementations of quantum walks have been reported in cold atoms [49, 50], NMR system [51, 52] and photonic systems [53–57]. DTQW implementations are ideally suited for lattice based quantum systems where lattice site represents the position space. DTQW is realised on ion-trap system by mapping position space to the motional phase space [58, 59]. However, implementation of quantum walks on quantum circuit is crucial to explore the practical realm of their algorithmic applications. The quantum circuit based implementation of DTQWs was first performed on a multi-qubit NMR system [52]. On any hardware, limitations in qubit number and coherence time restrict the number of steps that can be implemented. For implemention of DTQW on quantum circuit, one needs to map the position state to the multi-qubit state. Protocols using one such mapping on $N+1$-qutrits superconducting system to implement N-steps of DTQW has been reported [60]. Recently, an optimal form of quantum circuit for realization of DTQW on 5-qubit ion-trap quantum processor was presented and used for digital simulation of Dirac cellular automata [61]. Here we present a complete theory beyond the optimal form of quantum circuits that was used for realization of Dirac cellular automata.

In this paper, we review different forms of DTQWs and show their equivalence concerning physical implementations on quantum circuit. We also present various form of quantum circuits that can be realized on five qubit quantum processor for the implementation of one dimensional DTQWs. The circuits provided are for two variants of DTQW, standard QW and directed QW, respectively and that can be used to realize other forms of DTQW and Dirac cellular automata. They can be further scaled up and generalized to implement multi-particle DTQWs, and DTQW based algorithms.

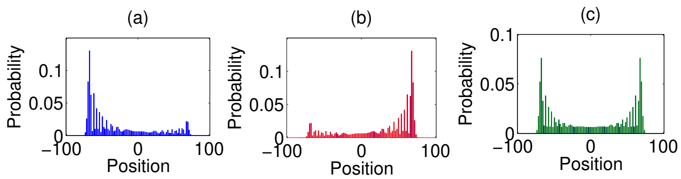

FIG. 1: Probability distribution after 100 time-steps of a standard DTQW (SQW) for different initial states with the coin parameter $\theta = \pi/4$. Initial states are $|\Psi_{in}\rangle = |\uparrow\rangle \otimes |x=0\rangle$ for (a), $|\Psi_{in}\rangle = |\downarrow\rangle \otimes |x=0\rangle$ for (b), and $|\Psi_{in}\rangle = \frac{1}{\sqrt{2}}(|\uparrow\rangle + |\downarrow\rangle) \otimes |x=0\rangle$ for (c). Alternate sites will have have zero probability in a SQW irrespective of the initial state.

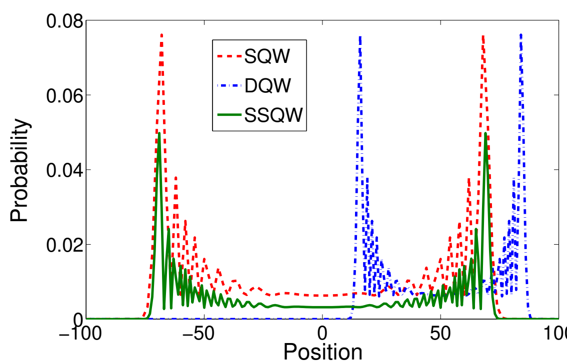

FIG. 2: Probability distribution for standard DTQW (SQW), directed DTQW (DQW), and split-step quantum walk (SSQW) with the coin parameter $\theta = \pi/4$ after 100-steps. In the plot, the zero probability value at alternate positions are discarded from the SQW. The spread in position space for the SQW and SSQW are identical but the peak values of the distribution are different. The spread is different for SQW and DQW, but their peak values are identical. The initial state is $|\Psi_{in}\rangle = \frac{1}{\sqrt{2}}(|\uparrow\rangle + |\downarrow\rangle) \otimes |x=0\rangle$ for all cases.

II. VARIANTS OF DTQW AND ITS EQUIVALENCE

A. Different forms of DTQW

DTQW is defined on the combination of particle (coin) and position Hilbert space $\mathcal{H} = \mathcal{H}_c \otimes \mathcal{H}_p$. Coin Hilbert space is defined by the particles internal states $\mathcal{H}_c = \text{span}\{|\uparrow\rangle, |\downarrow\rangle\}$ and one-dimensional position Hilbert space is spanned by $\mathcal{H}_p = \text{span}\{|x\rangle\}$, where $x \in \mathbb{Z}$ represents the labels on the position states. The generic initial state of the particle, $|\psi\rangle_c$, can be written as,

$$|\psi(\delta,\eta)\rangle_c = \cos(\delta)\,|\uparrow\rangle + e^{-i\eta}\sin(\delta)\,|\downarrow\rangle\,. \tag{1}$$

Each step of the walk evolves using a quantum coin operator acting on the particle space followed by a conditioned position shift operator acting on the entire Hilbert space. By modifying the coin and shift operators, different forms of DTQWs are achieved. The variants can have same coin operation but have different shift operation. The coin operator with single parameter is given by a rotation operator,

$$\hat{C}(\theta) = \begin{bmatrix} \cos(\theta) & -i\sin(\theta) \\ -i\sin(\theta) & \cos(\theta) \end{bmatrix} \otimes \mathcal{I}_l. \tag{2}$$

Here $\mathcal{I}_l$ is the identity operator on the position space of length l.

Standard DTQW (SQW) : Each step of SQW is realized by applying the operator, $\hat{W} = \hat{S}\hat{C}(\theta)$ where, coin operation for SQW is given by Eq. (2) and the conditioned position shift operator $\hat{S}$ is given by,

$$\hat{S} = \sum_{x\in\mathbb{Z}} \Big(|\uparrow\rangle\langle\uparrow| \otimes |x-1\rangle\langle x| + |\downarrow\rangle\langle\downarrow| \otimes |x+1\rangle\langle x| \Big). \tag{3}$$

The state of the particle in extended position space after t steps of SQW is given by,

$$|\Psi(t)\rangle = \hat{W}^t \Big[|\psi\rangle_c \otimes |x=0\rangle \Big] = \sum_{x=-t}^{t} \begin{bmatrix} \psi^{\uparrow}_{x,t} \\ \psi^{\downarrow}_{x,t} \end{bmatrix}. \tag{4}$$

The probability of finding the particle at position and time (x,t) is,

$$P(x,t) = \left\| \psi^{\uparrow}_{x,t} \right\|^2 + \left\| \psi^{\downarrow}_{x,t} \right\|^2. \tag{5}$$

Fig. 1 shows the probability distribution of a SQW for different initial states for $\theta = \pi/4$. The symmetry of the probability distribution naturally depends on the particular choice of the initial state of the walker. The symmetry and variance of the final distribution can also be affected by adding phases and thus taking advantage of the entire Bloch sphere for the coin operation in Eq. (2) [62].

Directed DTQW (DQW): On one-dimensional position space each step of DQW is evolved by applying coin operation as given by Eq. (2) on coin space followed by position shift operator $\hat{S}_d$ of the form,

$$\hat{S}_d = \sum_{x\in\mathbb{Z}} \Big(|\uparrow\rangle\langle\uparrow| \otimes |x\rangle\langle x| + |\downarrow\rangle\langle\downarrow| \otimes |x+1\rangle\langle x| \Big). \tag{6}$$

The shift operator at time t retains the particle at the existing position state or translates to the right conditioned on the internal state of the particle. Each step of the walk is realized by applying the operator, $\hat{W}_d = \hat{S}_d\hat{C}(\theta)$.

When the particle is in superposition of the internal state, during each step of the walk, some amplitude of the particle will simultaneously remain at the existing position state and translate to the right position state. In DQW, the spread of probability amplitude is over half position space than that of SQW.

Split-step DTQW (SSQW): In this variant, each step of the walk is a composition of two half-step evolutions,

$$\hat{W}_{ss} = \hat{S}_{+}\hat{C}(\theta)\hat{S}_{-}\hat{C}(\theta). \tag{7}$$

The single parameter coin operator is again given by Eq. (2) and the two shift operators have the form,

$$\hat{S}_{-} = \sum_{x\in\mathbb{Z}} \big(\left|\uparrow\right\rangle \left\langle\uparrow\right| \otimes \left|x-1\right\rangle \left\langle x\right| + \left|\downarrow\right\rangle \left\langle\downarrow\right| \otimes \left|x\right\rangle \left\langle x\right| \big) \tag{8a}$$

$$\hat{S}_{+} = \sum_{x\in\mathbb{Z}} \big(\left|\uparrow\right\rangle \left\langle\uparrow\right| \otimes \left|x\right\rangle \left\langle x\right| + \left|\downarrow\right\rangle \left\langle\downarrow\right| \otimes \left|x+1\right\rangle \left\langle x\right| \big). \tag{8b}$$

During each step of the SSQW, the particle remains at the same position and also moves to left and right positions conditioned on the internal state of the particle. This leads to a probability distribution that is different from the SQW. In addition to that, a different value of θ can be used for each half step giving additional control over the dynamics and probability distribution.

In Fig. 2 we show the probability distribution over position space after 100 steps of SQW, DQW and SSQW, respectively. The position space explored in the DQW is half the size compared to the SQW. The probability of finding the particle at each position space is non-zero for DQW when compared to SQW where the probability of finding particle at every alternate position is zero. Though the size of the position space is same for both, SSQW and SQW, but non-zero probability of finding the particle at all positions is seen in SSQW compared to SQW resulting in correspondingly lower peak values.

B. Equivalence of variants of discrete-time quantum walk

Among the three forms of the walk presented above, SSQW comprises both features, extended position states and non-zero probability at all positions. Therefore, one can consider SSQW as the most general form of a DTQW evolution. The state at any position x and time $(t+1)$ after the operation of $\hat{W}_{ss}$ at time t will be $\Psi_{x,t+1} = \psi^{\uparrow}_{x,t+1} + \psi^{\downarrow}_{x,t+1}$, where

$$\begin{aligned}\psi^{\uparrow}_{x,t+1} &= \cos(\theta)[\cos(\theta)\psi^{\uparrow}_{x+1,t} - i\sin(\theta)\psi^{\downarrow}_{x+1,t}] \\ &\quad - i\sin(\theta)[-i\sin(\theta)\psi^{\uparrow}_{x,t} + \cos(\theta)\psi^{\downarrow}_{x,t}]\end{aligned} \tag{9a}$$

$$\begin{aligned}\psi^{\downarrow}_{x,t+1} &= -i\sin(\theta)[\cos(\theta)\psi^{\uparrow}_{x,t} - i\sin(\theta)\psi^{\downarrow}_{x,t}] \\ &\quad + \cos(\theta)[-i\sin(\theta)\psi^{\uparrow}_{x-1,t} + \cos(\theta)\psi^{\downarrow}_{x-1,t}].\end{aligned} \tag{9b}$$

In the description below, we show that the amplitudes of the walker positions in the different quantum walk variants are identical after relabelling of the position state, which establishes that they are all equivalent.

Equivalence of SQW and SSQW: If we evolve two steps of SQW we will arrive at the state that is identical to Eq. (9) with only a replacement of $|x\pm1\rangle$ with $|x\pm2\rangle$. Without loss of generality we can show that,

$$\begin{aligned}\hat{W}_{ss} &\equiv \hat{W}^2 \\ \hat{S}_{+}\hat{C}(\theta)\hat{S}_{-}\hat{C}(\theta) &\equiv \Big[\hat{S}\hat{C}(\theta)\Big]^2\end{aligned} \tag{10}$$

where,

$$\begin{aligned}\hat{W}_{ss} &= \hat{S}_{+}\hat{C}(\theta)\hat{S}_{-}\hat{C}(\theta) \\ &= \Big[\Big(\cos^2\theta \left|\uparrow\right\rangle\left\langle\uparrow\right| - i\sin\theta\cos\theta\left|\uparrow\right\rangle\left\langle\downarrow\right|\Big) \otimes \sum \left|x-1\right\rangle\left\langle x\right| \\ &\quad + (-i\sin\theta\cos\theta\left|\downarrow\right\rangle\left\langle\uparrow\right| - \sin^2\theta\left|\downarrow\right\rangle\left\langle\downarrow\right|) \otimes \sum \left|x\right\rangle\left\langle x\right| \\ &\quad + (-\sin^2\theta\left|\uparrow\right\rangle\left\langle\uparrow\right| - i\sin\theta\cos\theta\left|\uparrow\right\rangle\left\langle\downarrow\right|) \otimes \sum \left|x\right\rangle\left\langle x\right| \\ &\quad + (-i\sin\theta\cos\theta\left|\uparrow\right\rangle\left\langle\downarrow\right| + \cos^2\theta\left|\downarrow\right\rangle\left\langle\downarrow\right|) \otimes \sum \left|x+1\right\rangle\left\langle x\right|\Big]\end{aligned} \tag{11}$$

and

$$\begin{aligned}\hat{W}^2 &= \hat{S}\hat{C}(\theta)\hat{S}\hat{C}(\theta) \\ &= \Big[(\cos^2\theta \left|\uparrow\right\rangle\left\langle\uparrow\right| - i\sin\theta\cos\theta\left|\uparrow\right\rangle\left\langle\downarrow\right|) \otimes \sum \left|x-2\right\rangle\left\langle x\right| \\ &\quad + (-i\sin\theta\cos\theta\left|\downarrow\right\rangle\left\langle\uparrow\right| - \sin^2\theta\left|\downarrow\right\rangle\left\langle\downarrow\right|) \otimes \sum \left|x\right\rangle\left\langle x\right| \\ &\quad + (-\sin^2\theta\left|\uparrow\right\rangle\left\langle\uparrow\right| - i\sin\theta\cos\theta\left|\uparrow\right\rangle\left\langle\downarrow\right|) \otimes \sum \left|x\right\rangle\left\langle x\right| \\ &\quad + (-i\sin\theta\cos\theta\left|\uparrow\right\rangle\left\langle\downarrow\right| + \cos^2\theta\left|\downarrow\right\rangle\left\langle\downarrow\right|) \otimes \sum \left|x+2\right\rangle\left\langle x\right|\Big].\end{aligned} \tag{12}$$

Equivalence shown in Eq. (10) can be established by mapping position space $|x\pm2\rangle$ to $|x\pm1\rangle$. Equivalence of Eq. (11) and Eq. (12) can also be obtained by using a modified version of the shift operators S'_{-} and S'_{+} where $|x\pm1\rangle$ in S_{-} and S_{+} [Eq. (8)] is replaced with $|x\pm2\rangle$. That is,

$$\hat{W}'_{ss} = \hat{S}'_{+}\hat{C}(\theta)\hat{S}'_{-}\hat{C}(\theta) = \Big[\hat{S}\hat{C}(\theta)\Big]^2. \tag{13}$$

Since the operator $\hat{W}_{ss} \equiv \hat{W}'_{ss} = \Big[\hat{S}\hat{C}(\theta)\Big]^2$, equivalance shown in Eq. (10) can be established and all the three operators will execute an identical transformation when applied on any initial state.

Equivalence of SQW and DQW : Two SQW steps are equivalent to two DQW steps followed by a translation operator which executes a global shift on the position space. For the choice of shift operator we have used,

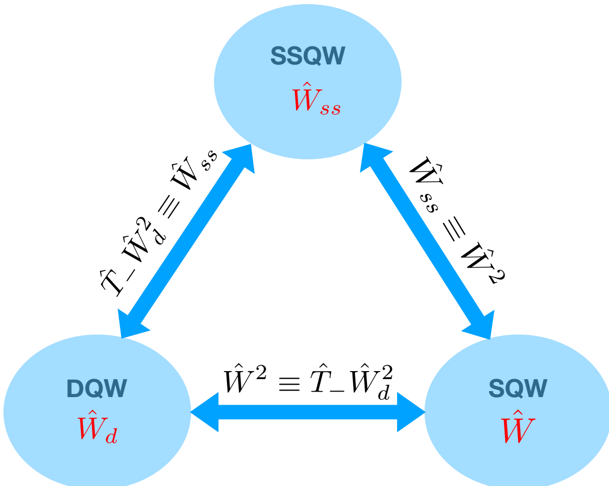

FIG. 3: Systematic presentation of the equivalence of the three forms of DTQW.

along with directed translation we can show that,

$$\hat{W}^2 \equiv \hat{T}_-{\hat{W}_d}^2$$
$$\left[\hat{S}\hat{C}(\theta)\right]^2 \equiv T_-\left[\hat{S}_d\hat{C}(\theta)\right]^2, \tag{14}$$

where, the form of $\hat{C}(\theta)$, $\hat{S}$, and $\hat{S}_d$ are given in Eqs. (2), (3), and (6), respectively and $\hat{T}_- = (\mathcal{I}_c \otimes \sum |x-1\rangle\langle x|)$. This can be explicitly shown by expanding the operators, $\hat{W}^2$ is given in Eq. (12) and

$$\begin{aligned}\hat{W}_{TD} &= \hat{T}_-{\hat{W}_d}^2 \\ &= \hat{T}_-\left[\hat{S}_d\hat{C}(\theta)\hat{S}_d\hat{C}(\theta)\right] \\ &= \Big[(\cos^2\theta\,|\uparrow\rangle\langle\uparrow| - i\sin\theta\cos\theta\,|\uparrow\rangle\langle\downarrow|) \otimes \sum|x-1\rangle\langle x| \\ &\quad + (-i\sin\theta\cos\theta\,|\downarrow\rangle\langle\uparrow| - \sin^2\theta\,|\downarrow\rangle\langle\downarrow|) \otimes \sum|x\rangle\langle x| \\ &\quad + (-\sin^2\theta\,|\uparrow\rangle\langle\uparrow| - i\sin\theta\cos\theta\,|\uparrow\rangle\langle\downarrow|) \otimes \sum|x\rangle\langle x| \\ &\quad + (-i\sin\theta\cos\theta\,|\uparrow\rangle\langle\downarrow| + \cos^2\theta\,|\downarrow\rangle\langle\downarrow|) \otimes \sum|x+1\rangle\langle x|\Big].\end{aligned} \tag{15}$$

By replacing $x \pm 2$ with $x \pm 1$ in Eq. (12) we can show that $\hat{W}_{TD} \equiv \hat{W}^2$. Therefore, for all physical realizations mapping the position space of the walker onto multi-qubit states of a quantum processor, one can ignore the alternate positions with zero probability in SQW. A resulting probability distribution is equivalent to the translated DQW.

Equivalence of SSQW and DQW: A SSQW as described by the operator $\hat{W}_{ss}$ is equal to two DQW steps described by $\hat{W}_d$ followed by a global translation operator of the form $\hat{T}_- = (\mathcal{I}_c \otimes \sum |x-1\rangle\langle x|)$. The probability distribution of $2t$- time steps of the directed walk is the same as the probability distribution of $t-$ steps of the split-step walk i.e.,

$$\hat{W}_{ss} = \hat{T}_-\hat{W}_d^2 \tag{16}$$

where $\hat{W}_{ss}$ and $\hat{W}_d$ are given in is given in Eq. (7) and Eq. (6), respectively. $\hat{T}_-\hat{W}_d^2$ is given in Eq. (15). Therefore, from Eq. (10), (14) and (16) we get,

$$\hat{W}_{ss} = \hat{T}_-\hat{W}_d^2 \equiv \hat{W}^2. \tag{17}$$

This implies that $\psi_{x\pm1}^{\uparrow(\downarrow)} = 0$, i.e., the position with zero probability in SQW. Thus, by discarding the positions with zero probability and relabelling values of position $x \pm 2$ as values of $x \pm 1$, the two-step SQW is equivalent to SSQW [63].

Schematic representation of the equivalence of all the three forms of DTQW is shown in Fig. 3 while Fig. 4 shows the probability distribution comparison for all the three forms of DTQW. The probability distribution of SSQW is equivalent to half of the time evolution of SQW and DQW. The probability values are the same for all three forms. Translation of DQW in position space recovers SSQW and discarding of position space with zero probability in SQW reduces its spread in position space and recovers SSQW.

Therefore, a quantum circuit which can implement one form of DTQW is sufficient to recover the exact probability distribution of the others by relabelling the position state associated with the multi-qubit state on the processor.

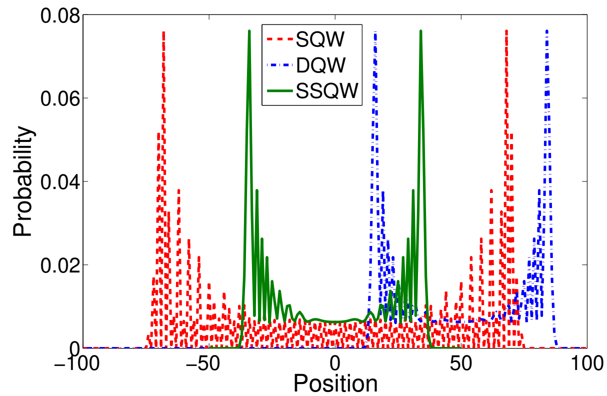

FIG. 4: Eqivalence of probability distribution for the different forms of DTQW, i.e., SQW and DQW for 100-steps and SSQW for 50 steps with the coin parameter $\theta = \pi/4$. Alternate sites of SQW have zero probability and thus 100-steps of SQW are equivalent to 50 time-steps of SSQW. The initial state is $|\Psi_{in}\rangle = \frac{1}{\sqrt{2}}(|\uparrow\rangle + |\downarrow\rangle) \otimes |x=0\rangle$.

III. QUANTUM CIRCUIT FOR IMPLEMENTING DTQW

To implement the DTQW on a quantum circuit in one dimensional position Hilbert space of size 2^N, $(N+1)$ qubits are needed. Among $(N+1)$ qubits, one qubit acts as coin and the states of the remaining qubits are mapped to the position states in DTQW. The basis for each qubit is characterized by its internal states $|0\rangle$ and $|1\rangle$. In principle, on 2^N position space, $(2^{N-1}-1)$-steps of SQW, and (2^N-1)-steps of DQW can be implemented.

Each step of SQW is evolved using a coin operation C_θ followed by the shift operation S as given in Eq. (3). Since S acts on the position state and the mapping of position to qubit state is not unique, therefore the composition of gates for the design of S is also not unique. The coin operation C_θ can be carried out by using a single qubit gate operation on the coin qubit, while the position-shift operation S can be subsequently applied with the help of multi-qubit gates where the coin qubit acts as the control. For instance, Fig. 5 presents a naive quantum circuit for single step of SQW on 5-qubit quantum processor [64]. The general form of this circuit depends on the mapping of the position state to the qubit states (see Table I).

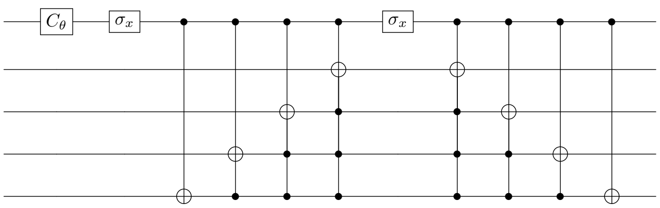

FIG. 5: Generic quantum circuit to implement one-step of SQW on a 5-qubit system for the mapping given in Table I. Repetition of this circuit will give us SQW on the position Hilbert space with 16-sites. The shift operation S is performed using increment and decrement circuit.

TABLE I: Mapping of position state to the multi-qubit state for quantum circuit presented in Fig. 5. This multi-qubit configuration identifies the even and odd position states in the system with the help of $|0\rangle$ and $|1\rangle$ as the state of the last qubit, respectively.

$\|x=0\rangle \equiv \|0000\rangle$	
$\|x=1\rangle \equiv \|0001\rangle$	$\|x=-1\rangle \equiv \|1111\rangle$
$\|x=2\rangle \equiv \|0010\rangle$	$\|x=-2\rangle \equiv \|1110\rangle$
$\|x=3\rangle \equiv \|0011\rangle$	$\|x=-3\rangle \equiv \|1101\rangle$
$\|x=4\rangle \equiv \|0100\rangle$	$\|x=-4\rangle \equiv \|1100\rangle$
$\|x=5\rangle \equiv \|0101\rangle$	$\|x=-5\rangle \equiv \|1011\rangle$
$\|x=6\rangle \equiv \|0110\rangle$	$\|x=-6\rangle \equiv \|1010\rangle$
$\|x=7\rangle \equiv \|0111\rangle$	$\|x=-7\rangle \equiv \|1001\rangle$

We can note that the mapping of position to qubit state is not unique and the quantum circuit can be simplified using different mapping. Here the odd (or even) position state is identified with the configuration of last qubit $|1\rangle$ (or $|0\rangle$). Repeating the circuit in Fig. 5, will give 7-steps of SQW but it can be scaled to N-qubit using increment and decrement circuit. However, for this mapping the gate size and gate counting per step of SQW increases with the number of qubits. At this point, we have claimed that the quantum circuit complexity of DTQW depends on the position space mapping. Therefore, we will now show that a mapping that takes the architecture of the quantum processor into account reduce the gate size and gate count. Additional reductions can be achieved by fixing the initial state of the walk. Here, we present quantum circuit on five-qubit system for SQW and DQW that can be easily realised on present day quantum processors e.g., the five qubit programmable trapped-ion quantum computer [61] or on IBMQ's five qubit quantum computer [65, 66].

TABLE II: Mapping of position state to the multi-qubit state for quantum circuits presented in Figs. 6, 7, 8, and 9. Here, also the multi-qubit configuration identifies even and odd numbered positions in the system with respect to $|0\rangle$ and $|1\rangle$ state of the last qubit, respectively.

$\|x=0\rangle \equiv \|0000\rangle$	
$\|x=1\rangle \equiv \|0001\rangle$	$\|x=-1\rangle \equiv \|0011\rangle$
$\|x=2\rangle \equiv \|0110\rangle$	$\|x=-2\rangle \equiv \|0010\rangle$
$\|x=3\rangle \equiv \|0111\rangle$	$\|x=-3\rangle \equiv \|0101\rangle$
$\|x=4\rangle \equiv \|1100\rangle$	$\|x=-4\rangle \equiv \|0100\rangle$
$\|x=5\rangle \equiv \|1101\rangle$	$\|x=-5\rangle \equiv \|1111\rangle$
$\|x=6\rangle \equiv \|1010\rangle$	$\|x=-6\rangle \equiv \|1110\rangle$
$\|x=7\rangle \equiv \|1011\rangle$	$\|x=-7\rangle \equiv \|1001\rangle$

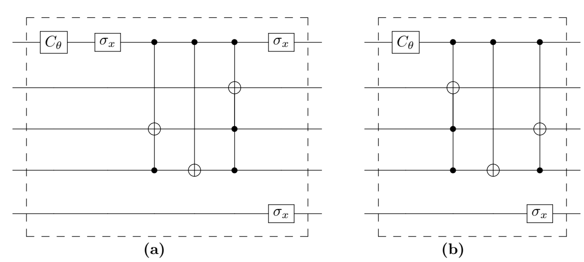

FIG. 6: Generic quantum circuit for two steps of SQW on a 5-qubit system for the mapping given in table II. It can be used to implement up to seven steps of SQW by alternating circuit (a) and (b). If the initial position-state is even, circuit (a) is applied first, and if the initial position-state is odd circuit (b) is applied first.

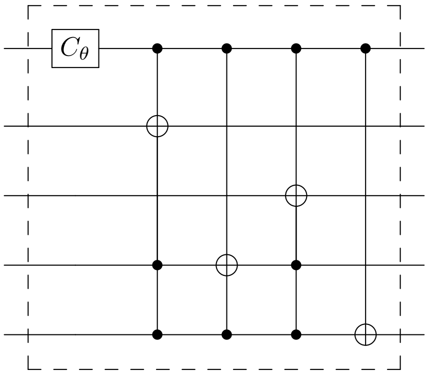

FIG. 7: Generic quantum circuit for a DQW on 5-qubit system for the mapping given in table II. Concatenation of this circuit will give the probability distribution of DQW for upto 15-steps.

TABLE III: Mapping of position state to the multi-qubit state for quantum circuits presented in Fig. 10 and Fig. 11.

$\|x = 0\rangle \equiv \|0000\rangle$	
$\|x = 1\rangle \equiv \|0001\rangle$	$\|x = -1\rangle \equiv \|0111\rangle$
$\|x = 2\rangle \equiv \|0010\rangle$	$\|x = -2\rangle \equiv \|0110\rangle$
$\|x = 3\rangle \equiv \|0011\rangle$	$\|x = -3\rangle \equiv \|0101\rangle$
$\|x = 4\rangle \equiv \|1100\rangle$	$\|x = -4\rangle \equiv \|0100\rangle$
$\|x = 5\rangle \equiv \|1101\rangle$	$\|x = -5\rangle \equiv \|1011\rangle$
$\|x = 6\rangle \equiv \|1110\rangle$	$\|x = -6\rangle \equiv \|1010\rangle$
$\|x = 7\rangle \equiv \|1111\rangle$	$\|x = -7\rangle \equiv \|1001\rangle$

Fig. 6, shows quantum circuit for two-steps of SQW for the mapping presented in table II. Similar to the previous case, the state of the last qubit defines the even and odd positions. This allows us to keep the rest of the qubits mapped identical for each pair of even and odd positions. For a generic initial position state $|x\rangle$ of the particle on a five-qubit system, the alternation of circuit **(a)** and **(b)**, as given in Fig. 6, implements the seven steps of SQW. If the initial position $|x\rangle$ is even (or odd), circuit **(a)** (or **(b)**) is applied first. When compared to the quantum circuit in Fig. 5 for a naive mapping, we see a significant decrease in gate count and gate size for each step. The gate count reduces to almost half for each step. Similarly, Fig. 7 shows quantum circuit for each step of DQW for mapping presented in table II for any arbitrary initial position state $|x\rangle$ and by repeated application of this circuit, one can implement 15-steps of DQW, in principle.

On comparison of the two quantum circuit for SQW, one step of naive mapping shown in Fig. 5 has double of each Toffoli-3 gate, Toffoli-2 gate, Toffoli gate and CNOT gate along with three single qubit gates, respectively while each step of generic circuit shown in Fig. 6 for mapping in table II has only one Toffoli-2 gate, one Toffoli gate and one CNOT gate along with few single qubit gates. Hence, this shows that for a smart position state mapping, the gate count drops significantly and hence the circuit complexity reduces.

Fixing the initial state of the walker helps in reducing the gate count in the quantum circuit and also reduces the circuit complexity. For example, if the initial state is fixed to $|0\rangle \otimes |0000\rangle \equiv |\uparrow\rangle \otimes |x = 0\rangle$ then the quantum circuit for first seven steps of SQW and DQW is shown in Fig. 8 and Fig. 9, respectively. But for the implementation of SSQW, two different shift operators are needed. The same results can be reconstructed from the equivalence relation between SSQW and SQW, which will need two steps of SQW to reproduce the results of SSQW. Therefore, using SQW and reconstructing the results of the corresponding SSQW from it is more efficient than the direct implementation of SSQW.

We have also considered a different configuration of position space mapping onto multi-qubit states. As in table II the last qubit states $|0\rangle$ and $|1\rangle$ are set to identify the even and odd position of the position state here too. The mapping shown in table III and Fig. 10 and 11 shows the quantum circuits for SQW and DQW for the mapping choices, respectively, which implements seven steps for the initial state $|0\rangle \otimes |x = 0\rangle$. At alternate sites of the SQW we have zero probability, and our mapping allows the value of the last qubit to identify odd or even positions. Alternatively, the step number can be classically tracked in the quantum circuits shown in Fig. 6, 8 and 10 to reduce the number of σ_x operations on the last qubit to zero or one.

Among the quantum circuits presented, the one given in Fig. 8 is optimal for implementing the SQW. Although table IV gives a comparison of the number of gates in the optimized circuits in Fig. 8, 9, 10 and 11, respectively.

TABLE IV: Gate count for mapping in Table II and III, respectively and for corresponding SQW and DQW circuits with fixed initial state $|0\rangle \otimes |0000\rangle$ and after seven steps on five-qubit quantum processor.

	SQW	DQW
Table II	22 single-qubit 7 two-qubit 6 three-qubit 4 four-qubit	7 single-qubit 7 two-qubit 6 three-qubit 10 four-qubit
Table III	22 single-qubit 8 two-qubit 6 three-qubit 4 four-qubit	7 single-qubit 6 two-qubit 6 three-qubit 8 four-qubit

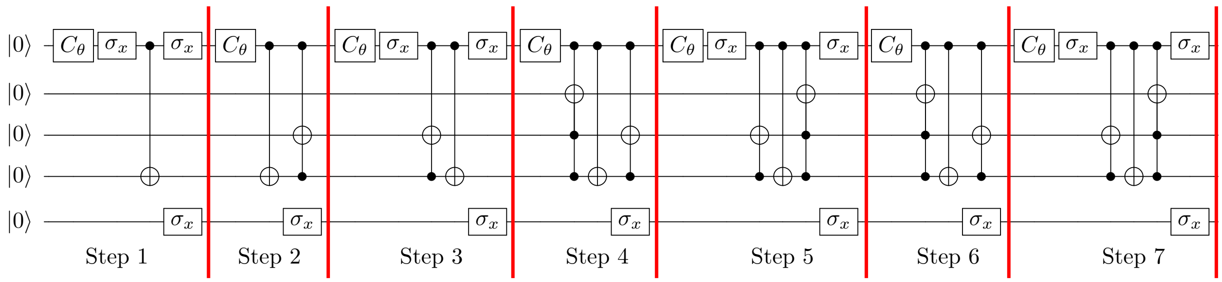

FIG. 8: Quantum circuit for first seven steps of the SQW on a 5-qubit system with a fixed initial state $|\uparrow\rangle \otimes |x = 0\rangle \equiv |0\rangle \otimes |0000\rangle$ for the mapping given in table II. This circuit has a reduced gate count compared to the generic circuit shown in Fig. 6. We note that the sequence of σ_x in the last qubit can be replaced by classically tracking the number of steps.

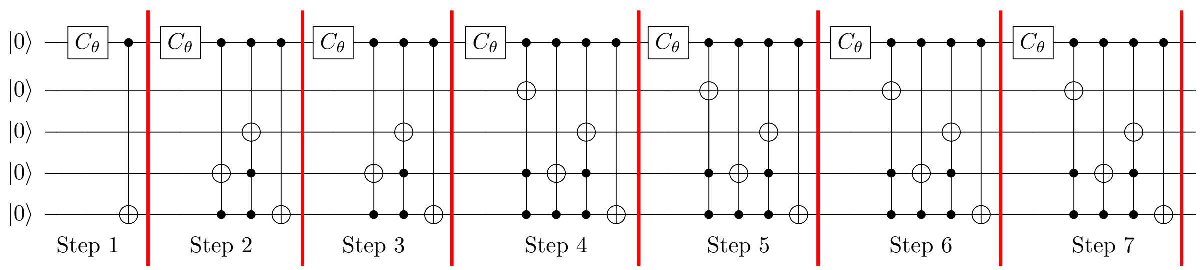

FIG. 9: Quantum circuit for first seven steps of the DQW on a 5-qubit system with a fixed initial state $|\uparrow\rangle \otimes |x = 0\rangle \equiv |0\rangle \otimes |0000\rangle$ for the mapping given in table II. It has reduced gate count compared to the generic circuit shown in Fig. 7.

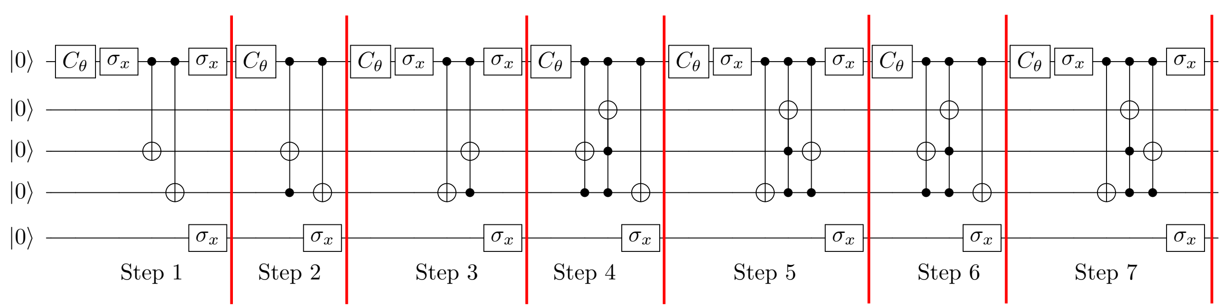

FIG. 10: Quantum circuit for SQW for the first seven steps on 5-qubit system for the fixed initial state $|\uparrow\rangle \otimes |x = 0\rangle \equiv |0\rangle \otimes |0000\rangle$ for the mapping given in table III. Here also, the sequence of σ_x in the last qubit can be completely replaced by classical tracking the step-number.

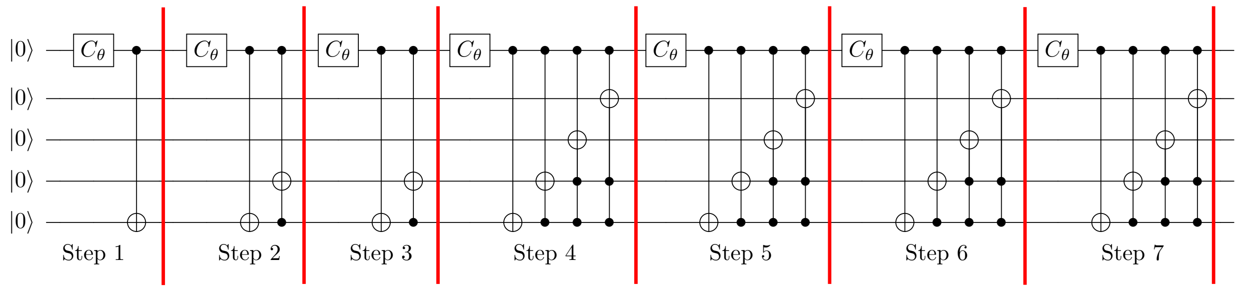

FIG. 11: Quantum circuit for first seven steps of the DQW on a 5-qubit system with a fixed initial state $|\uparrow\rangle \otimes |x=0\rangle \equiv |0\rangle \otimes |0000\rangle$ for the mapping given in table III.

IV. DISCUSSION

By digitally encoding the walker's position space onto qubits state in various ways, we have shown different equivalent quantum walk circuits. The examples illustrate how the encoding methods and initial state dependent circuits can reduce the required gate depth (gate count) for implementing quantum walks.

The circuits can be scaled to implement more number of steps on a larger system using higher order Toffoli gates. The implementation of n steps of a SQW will need at least $(\log_2(n+1)+2)$ qubits. Similarly, for implementing n steps of a DQW, at least $(\log_2(n+1)+1)$ qubits are required.

Recently, different ways of expanding the incrementing and decrementing part of the generic quantum circuit show in Fig.5 was explored in detail [67]. To reduce the circuit complexity, generalized controlled inversions approach and the other one by effectively replacing them with rotation operations around the basis states was presented. If the circuits are implemented on a device with large number of qubits then generalised controlled inversions would be a good option as it has less circuit depth due to the use of ancilla qubits or else the other way would be better. In our work the focus has been on reducing the circuit complexity by careful choice of mapping of qubit state to the position space and optimizing the circuit after choosing the initial state. Combining both these approaches may results in further reduction of circuit complexity and that needs to be carefully explored in future works.

DTQW in two-dimensional position space [68, 69], can also be implemented by scaling the scheme presented in work with an appropriate mapping of qubit states with the nearest neighbour position space in both dimensions. It can be achieved on a device with access to larger number of qubits. By assigning the equal number of qubits to both the dimensions in the two-dimensional position space and then by optimally mapping the qubit state to the position state. All the circuits presented can be extended to implement two or more particle DTQWs by introducing two or more coin qubits into the system, respectively. In such cases, the control over the target or position qubit increases with the number of coin qubits. Another way of scaling the scheme for SQW on a N-qubit system, one can fix one-qubit for coin as usual and another one to represent the $\pm$-sign for the positive and negative direction of the initial state $|x\rangle$ and the state of the rest of the $(N-2)$ qubit can be mapped to position state. Now using the quantum adder circuit [70], the scheme can be extended to N-qubits and a generalized quantum circuit for quantum walk can be worked out.

One can also use ancilla qubits to reduce the circuit complexity. In the appendix, we have shown a hybrid-circuit with the help ancilla qubit for DQW. DQW can be implemented with the help of CNOT gate and interference in the walk can be included with help of controlled-SWAP gate and ancilla qubit just before the measurement. Fig. 14 and 15 shows the hybrid circuit for three-steps and four-steps of DQW. Detail is given in the Apendix.

Therefore, with an appropriate choice of quantum coin operation and the equivalence of variants of DTQW, any quantum algorithm based on DTQW can be experimentally realized on quantum computer. Dirac cellular automata can be recovered using SSQW, which reproduces the dynamics of the Dirac equation in the continuum limit [41]. One such example of simulating Dirac cellular automata on an ion-trap processor using one of the various configurations of the circuits presented has been demonstrated recently [71]. With the appropriate use of position dependent coin operation and additional higher order Toffoli gates to our circuits, other DTQW based algorithms, such as spatial search can also be implemented.

Acknowledgement:

CHA acknowledges financial support from CONACYT doctoral grant no. 455378. NML acknowledges financial support from the NSF grant no. PHY-1430094 to the PFC@JQI. CMC acknowledge the support from the Department of Science and Technology, Government of India under Ramanujan Fellowship grant no. SB/S2/RJN-192/2014 and US Army ITC-PAC grant no. FA520919PA139.

[1] J. Preskill, “Quantum computing in the nisq era and beyond,” *Quantum*, vol. 2, p. 79, 2018.

[2] Y. Alexeev *et al.*, ”Quantum Computer Systems for Scientific Discovery,” arXiv 1912.07577 (2019)

[3] J. Kempe, “Quantum random walks: an introductory overview,” *Contemporary Physics*, vol. 44, no. 4, pp. 307–327, 2003.

[4] S. E. Venegas-Andraca, “Quantum walks: a comprehensive review,” *Quantum Information Processing*, vol. 11, no. 5, pp. 1015–1106, 2012.

[5] A. M. Childs, R. Cleve, E. Deotto, E. Farhi, S. Gutmann, and D. A. Spielman, “Exponential algorithmic speedup by a quantum walk,” in *Proceedings of the thirty-fifth annual ACM symposium on Theory of computing*, pp. 59–68, ACM, 2003.

[6] A. Ambainis, “Quantum walks and their algorithmic applications,” *International Journal of Quantum Information*, vol. 1, no. 04, pp. 507–518, 2003.

[7] N. Shenvi, J. Kempe, and K. B. Whaley, “Quantum random-walk search algorithm,” *Physical Review A*, vol. 67, no. 5, p. 052307, 2003.

[8] A. Ambainis, “Quantum walk algorithm for element distinctness,” *SIAM Journal on Computing*, vol. 37, no. 1, pp. 210–239, 2007.

[9] F. Magniez, M. Santha, and M. Szegedy, “Quantum algorithms for the triangle problem,” *SIAM Journal on Computing*, vol. 37, no. 2, pp. 413–424, 2007.

[10] B. L. Douglas and J. B. Wang, “A classical approach to the graph isomorphism problem using quantum walks,” *Journal of Physics A: Mathematical and Theoretical*, vol. 41, no. 075303, 2008.

[11] J. K. Gamble, M. Friesen, D. Zhou, R. Joynt, and S. Coppersmith, “Two-particle quantum walks applied to the graph isomorphism problem,” *Physical Review A*, vol. 81, no. 5, 2010.

[12] S. D. Berry and J. B. Wang, “Two-particle quantum walks: Entanglement and graph isomorphism testing,” *Physical Review A*, vol. 83, no. 4, 2011.

[13] G. D. Paparo and M. Martin-Delgado, “Google in a quantum network,” *Scientific reports*, vol. 2, p. 444, 2012.

[14] G. D. Paparo, M. Müller, F. Comellas, and M. A. Martin-Delgado, “Quantum google in a complex network,” *Scientific reports*, vol. 3, p. 2773, 2013.

[15] T. Loke, J. Tang, J. Rodriguez, M. Small, and J. B. Wang, “Comparing classical and quantum pageranks,” *Quantum information processing*, vol. 16, no. 1, p. 25, 2017.

[16] C. M. Chandrashekar, Prateek Chawla, Roopesh Mangal, “Discrete-time quantum walk algorithm for ranking nodes on a network,” *arXiv*, no. 1905.06575, 2019.

[17] P. Arrighi, S. Facchini, and M. Forets, “Quantum walking in curved spacetime,” *Quantum Information Processing*, vol. 15, no. 8, pp. 3467–3486, 2016.

[18] G. Di Molfetta, M. Brachet, and F. Debbasch, “Quantum walks in artificial electric and gravitational fields,” *Physica A: Statistical Mechanics and its Applications*, vol. 397, pp. 157–168, 2014.

[19] G. Di Molfetta, M. Brachet, and F. Debbasch, “Quantum walks as massless dirac fermions in curved space-time,” *Physical Review A*, vol. 88, no. 4, p. 042301, 2013.

[20] C. M. Chandrashekar, “Two-component Dirac-like Hamiltonian for generating quantum walk on one-, two- and three-dimensional lattices,” *Scientific reports*, vol. 3, p. 2829, 2013.

[21] C. M. Chandrashekar, S. Banerjee, and R. Srikanth, “Relationship between quantum walks and relativistic quantum mechanics,” *Physical Revimore than double of each of the multi-qubit gate than compared toew A*, vol. 81, no. 6, p. 062340, 2010.

[22] F. W. Strauch, “Relativistic quantum walks,” *Physical Review A*, vol. 73, no. 5, p. 054302, 2006.

[23] G. Di Molfetta and A. Pérez, “Quantum walks as simulators of neutrino oscillations in a vacuum and matter,” *New Journal of Physics*, vol. 18, no. 10, p. 103038, 2016.

[24] A. Mallick, S. Mandal, A. Karan, and C. M. Chandrashekar, “Simulating Dirac Hamiltonian in curved space-time by split-step quantum walk,” *Journal of Physics Communications* 3 (1), 015012, 2019.

[25] C. M. Chandrashekar and T. Busch, “Localized quantum walks as secured quantum memory,” *EPL (Europhysics Letters)*, vol. 110, no. 1, p. 10005, 2015.

[26] A. Mallick, S. Mandal, and C. M. Chandrashekar, “Neutrino oscillations in discrete-time quantum walk framework,” *The European Physical Journal C*, vol. 77, no. 2, p. 85, 2017.

[27] D. Aharonov, A. Ambainis, J. Kempe, and U. Vazirani, “Quantum walks on graphs,” pp. 50–59, 2001.

[28] B. Tregenna, W. Flanagan, R. Maile, and V. Kendon, “Controlling discrete quantum walks: coins and initial states,” *New Journal of Physics*, vol. 5, no. 1, p. 83, 2003.

[29] E. Farhi and S. Gutmann, “Quantum computation and decision trees,” *Physical Review A*, vol. 58, no. 2, p. 915, 1998.

[30] H. Gerhardt and J. Watrous, “Continuous-time quantum walks on the symmetric group,” pp. 290–301, 2003.

[31] G. V. Ryazanov, “The feynman path integral for the dirac equation,” *JETP*, vol. 6, no. 6, pp. 1107–1113, 1958.

[32] R. P. Feynman, “Quantum mechanical computers,” *Foundations of physics*, vol. 16, no. 6, pp. 507–531, 1986.

[33] K. R. Parthasarathy, “The passage from random walk to diffusion in quantum probability,” *Journal of Applied Probability*, vol. 25, pp. 151–166, 1988.

[34] Y. Aharonov, L. Davidovich, and N. Zagury, “Quantum random walks,” *Physical Review A*, vol. 48, no. 2, p. 1687, 1993.

[35] A. M. Childs, R. Cleve, E. Deotto, E. Farhi, S. Gutmann, and D. A. Spielman, “Exponential algorithmic speedup by a quantum walk,” in *Proceedings of the thirty-fifth annual ACM symposium on Theory of computing*, pp. 59–68, ACM, 2003.

[36] S. Hoyer and D. A. Meyer, “Faster transport with a directed quantum walk,” *Physical Review A*, vol. 79, no. 2,

p. 024307, 2009.

[37] A. Montanaro, "Quantum walks on directed graphs," *arXiv preprint quant-ph/0504116*, 2005.

[38] C. M. Chandrashekar and T. Busch, "Quantum percolation and transition point of a directed discrete-time quantum walk," *Scientific reports*, vol. 4, p. 6583, 2014.

[39] T. Kitagawa, M. A. Broome, A. Fedrizzi, M. S. Rudner, E. Berg, I. Kassal, A. Aspuru-Guzik, E. Demler, and A. G. White, "Observation of topologically protected bound states in photonic quantum walks," *Nature communications*, vol. 3, p. 882, 2012.

[40] J. K. Asbóth, "Symmetries, topological phases, and bound states in the one-dimensional quantum walk," *Physical Review B*, vol. 86, no. 19, p. 195414, 2012.

[41] A. Mallick and C. M. Chandrashekar, "Dirac cellular automaton from split-step quantum walk," *Scientific Reports*, vol. 6, p. 25779, 2016.

[42] M. Szegedy, "Quantum speed-up of markov chain based algorithms," in *Foundations of Computer Science, 2004. Proceedings. 45th Annual IEEE Symposium on*, pp. 32–41, IEEE, 2004.

[43] D. A. Meyer, "From quantum cellular automata to quantum lattice gases," *Journal of Statistical Physics*, vol. 85, no. 5-6, pp. 551–574, 1996.

[44] A. Pérez, "Asymptotic properties of the dirac quantum cellular automaton," *Physical Review A*, vol. 93, no. 1, p. 012328, 2016.

[45] C. M. Chandrashekar, "Disorder induced localization and enhancement of entanglement in one- and two-dimensional quantum walks," *arXiv preprint arXiv:1212.5984*, 2012.

[46] A. Joye, "Dynamical localization for d-dimensional random quantum walks," *Quantum Information Processing*, vol. 11, no. 5, pp. 1251–1269, 2012.

[47] H. Obuse and N. Kawakami, "Topological phases and delocalization of quantum walks in random environments," *Physical Review B*, vol. 84, no. 19, p. 195139, 2011.

[48] T. Kitagawa, M. S. Rudner, E. Berg, and E. Demler, "Exploring topological phases with quantum walks," *Physical Review A*, vol. 82, no. 3, p. 033429, 2010.

[49] H. B. Perets, Y. Lahini, F. Pozzi, M. Sorel, R. Morandotti, and Y. Silberberg, "Realization of quantum walks with negligible decoherence in waveguide lattices," *Physical review letters*, vol. 100, no. 17, p. 170506, 2008.

[50] M. Karski, L. Förster, J.-M. Choi, A. Steffen, W. Alt, D. Meschede, and A. Widera, "Quantum walk in position space with single optically trapped atoms," *Science*, vol. 325, no. 5937, pp. 174–177, 2009.

[51] J. Du, H. Li, X. Xu, M. Shi, J. Wu, X. Zhou, and R. Han, "Experimental implementation of the quantum random-walk algorithm," *Physical Review A*, vol. 67, no. 042316, 2003

[52] C. A. Ryan, M. Laforest, J.-C. Boileau, and R. Laflamme, "Experimental implementation of a discrete-time quantum random walk on an nmr quantum-information processor," *Physical Review A*, vol. 72, no. 6, p. 062317, 2005.

[53] A. Schreiber, K. N. Cassemiro, V. Potoček, A. Gábris, P. J. Mosley, E. Andersson, I. Jex, and C. Silberhorn, "Photons walking the line: a quantum walk with adjustable coin operations," *Physical review letters*, vol. 104, no. 5, p. 050502, 2010.

[54] A. Peruzzo, M. Lobino, J. C. Matthews, N. Matsuda, A. Politi, K. Poulios, X.-Q. Zhou, Y. Lahini, N. Ismail, K. Wörhoff, *et al.*, "Quantum walks of correlated photons," *Science*, vol. 329, no. 5998, pp. 1500–1503, 2010.

[55] M. A. Broome, A. Fedrizzi, B. P. Lanyon, I. Kassal, A. Aspuru-Guzik, and A. G. White, "Discrete single-photon quantum walks with tunable decoherence," *Physical Review Letters*, vol. 104, no. 15, p. 153602, 2010.

[56] X. Qiang, T. Loke, A. Montanaro, K. Aungskunsiri, X. Zhou, J. L. OBrien, J. B. Wang, and J. C. F. Matthews, "Efficient quantum walk on a quantum processor," *Nat Commun*, vol. 7, no. 11511, 2016.

[57] X. Qiang, X. Zhou, J. Wang, C. M. Wilkes, T. Loke, S. OGara, L. Kling, G. D. Marshall, R. Santagati, T. C. Ralph, J. B. Wang, J. L. OBrien, M. G. Thompson, and J. C. F. Matthews, "Large-scale silicon quantum photonics implementing arbitrary two-qubit processing," *Nature Photon*, vol. 12, p. 534539, 2018.

[58] H. Schmitz, R. Matjeschk, C. Schneider, J. Glueckert, M. Enderlein, T. Huber, and T. Schaetz, "Quantum walk of a trapped ion in phase space," *Physical review letters*, vol. 103, no. 9, p. 090504, 2009.

[59] F. Zähringer, G. Kirchmair, R. Gerritsma, E. Solano, R. Blatt, and C. Roos, "Realization of a quantum walk with one and two trapped ions," *Physical review letters*, vol. 104, no. 10, p. 100503, 2010.

[60] J.-Q. Zhou, L. Cai, Q.-P. Su, and C.-P. Yang, "Protocol of a quantum walk in circuit QED," *Physical Review A*, vol. 100, no. 1, p. 012343, 2019.

[61] S. Debnath, N. M. Linke, C. Figgatt, K. A. Landsman, K. Wright, and C. Monroe, "Demonstration of a small programmable quantum computer with atomic qubits" *Nature* vol. 536, no. 63, 2016.

[62] C. M. Chandrashekar, R. Srikanth, and R. Laflamme, "Optimizing the discrete-time quantum walk using SU(2) coin" *Physical Rev A*, vol. 77, 032326, 2008.

[63] N. P. Kumar, R. Balu, R. Laflamme, and C. M. Chandrashekar, "Bounds on the dynamics of periodic quantum walks and emergence of the gapless and gapped dirac equation," *Physical Review A*, vol. 97, no. 1, p. 012116, 2018.

[64] B. Douglas and J. Wang, "Efficient quantum circuit implementation of quantum walks," *Physical Review A*, vol. 79, no. 5, p. 052335, 2009.

[65] F. Acasiete, F. P. Agostini, J. K. Moqadam and R. Portugal, "Implementation of quantum walks on IBM quantum computers ", *QIP*, vol. 19, 426, 2020.

[66] The IBM Quantum Experience, *http://www.research.ibm.com/quantum*.

[67] K. Georgopoulos, C. Emary, and P. Zuliani, "Comparison of quantum-walk implementations on noisy intermediate-scale quantum computers," *Physical Review A*, vol. 103, no. 2, p. 022408, 2021.

[68] C. Di Franco, M. Mc Gettrick, and Th. Busch, "Mimicking the Probability Distribution of a Two-Dimensional Grover Walk with a Single-Qubit Coin," *Phys. Rev. Lett.* **106**, 080502, 2011.

[69] C. M. Chandrashekar, Th. Busch, "Decoherence on a two-dimensional quantum walk using four- and two-state particle," *J. Phys. A: Math. Theor.* vol. 46, 105306, 2013.

[70] Kai-Wen Cheng and Chien-Cheng Tseng, *Electronics Letters*, vol. 38, Issue 22, p. 1343 - 1344, 2002.

[71] C. H.Alderete, S. Singh, N. H. Nguyen, D. Zhu, R. Balu, C. Monroe, C. M. Chandrashekar and N. M. Linke , "Quantum walks and Dirac cellular automata on a programmable trapped-ion quantum computer," *Nat. Com-*

mun., vol. 11, 3720 (2020).
[72] K. A. Landsman, C. Figgatt, T. Schuster, N. M. Linke, B. Yoshida, N. Y. Yao, and C. Monroe, “Verified quantum information scrambling,” *Nature*, vol. 567, no. 7746, p. 61, 2019.
[73] J. Zhang, G. Pagano, P. W. Hess, A. Kyprianidis, P. Becker, H. Kaplan, A. V. Gorshkov, Z.-X. Gong, and C. Monroe, “Observation of a many-body dynamical phase transition with a 53-qubit quantum simulator,” *Nature*, vol. 551, no. 7682, p. 601, 2017.
[74] J. G. Bohnet, B. C. Sawyer, J. W. Britton, M. L. Wall, A. M. Rey, M. Foss-Feig, and J. J. Bollinger, “Quantum spin dynamics and entanglement generation with hundreds of trapped ions,” *Science*, vol. 352, no. 6291, pp. 1297–1301, 2016.
[75] Z. Yan, Y.-R. Zhang, M. Gong, Y. Wu, Y. Zheng, S. Li, C. Wang, F. Liang, J. Lin, Y. Xu, *et al.*, “Strongly correlated quantum walks with a 12-qubit superconducting processor,” *Science*, vol. 364, no. 6442, pp. 753–756, 2019.
[76] J. A. Smolin, and D. P. DiVincenzo, ”Five two-bit quantum gates are sufficient to implement the quantum Fredkin gate” *Physical Review A*, vol. 53, no. 4, p. 2855, 1996.
[77] M. A. Nielsen, and I. L. Chuang, ”Quantum Computation and Quantum Information” *First edition* (2000).
[78] A. D. Corcoles, E. Magesan, S. J. Srinivasan, A. W. Cross, M. Steffen, J. M. Gambetta, and J. M. Chow, ”Demonstration of a quantum error detection code using a square lattice of four superconducting qubit” *Nature Communications*, vol. 6, no. 6979, 2015.
[79] W. Huggins, P. Patil, B. Mitchell, K. B. Whaley, and E. M. Stoudenmir, ”Towards quantum machine learning with tensor networks,” *Quantum Science and Technology*, **4**, 2, 2019.

Appendix

DQW circuit with naive mapping

A naive mapping can result in an inefficient quantum circuit. One example of this is given in table V and Fig. 12.

TABLE V: Mapping of position state onto multi-qubit states for DQW circuit presented in Fig. 12.

$\|x=0\rangle \equiv \|0000\rangle$	
$\|x=1\rangle \equiv \|1000\rangle$	$\|x=4\rangle \equiv \|1111\rangle$
$\|x=2\rangle \equiv \|1100\rangle$	$\|x=5\rangle \equiv \|0111\rangle$
$\|x=3\rangle \equiv \|1110\rangle$	$\|x=6\rangle \equiv \|1011\rangle$

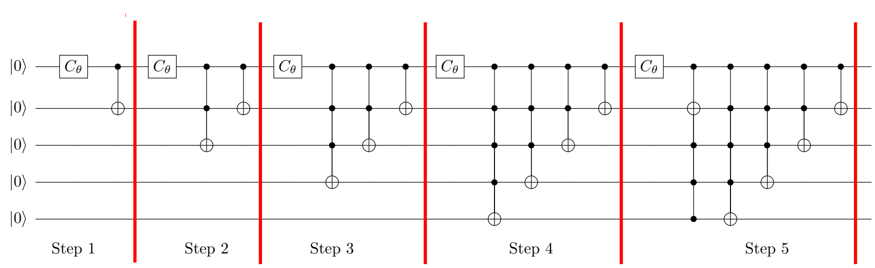

FIG. 12: Quantum circuit for DQW for first five steps with the fixed initial state $|\Psi_{in}\rangle = |\uparrow\rangle \otimes |x=0\rangle \equiv |0\rangle \otimes |0000\rangle$ for the naive mapping shown in table V. This circuit has a simple structure but it consists of many additional higher order Toffoli gates compared to the circuits shown in Sec. III and Appendix.

The simplest quantum circuit for the mapping given above with fixed initial state, $|0\rangle \otimes |0000\rangle$ is shown in Fig. 12. This circuit implements five steps of the DQW. In the same system one can implement upto 15 steps since the available position states are $2^4 = 16$. This circuit looks straightforward to construct and scale but an actual implementation would require higher-order Toffoli gates even for a small number of steps and fixed initial position, making it inefficient for near term quantum processors.

Simplified quantum circuit with ancilla

There has been a significant increase in the number of qubits available on platforms like trapped ion and superconducting qubits [72–75]. However, limited coherence time is still an hindrance to increase the number of gates that can be implemented. To make an explicit use of the all available qubits, one has to develop a low depth quantum circuits. Here we will present quantum circuits with reduced number of gates to implement DQWs at the cost of requiring additional ancilla qubits. But the given circuit is still inefficient as it will only include outputs with ancilla qubit state $|0\rangle$. In a system with access to more qubits, one can implement more steps of the DQW at the same circuit depth but the efficiency decreases as the number of output states that can be included is when all the ancilla qubit state is $|0\rangle$.

For a five qubit system, we again use the first qubit to represent the coin and the other four qubits to represent position space. The mapping is given in table VI. This is a classical circuit as it does not include the superposition or interference in the system directly. The output of the DQW and that of the quantum circuit in Fig. 13 is compared in table VII for each step. To keep track of the contribution from each time evolution, we have introduced subscript to indicate different time steps. To turn this circuit into a DQW implementation, CNOT, Fredkin (controlled-Swap) gates and a Hadamard gate involving additional ancilla qubits are applied before measurement as shown in Fig. 15. After measurement only selective outputs with ancilla qubit state $|0\rangle$ are included.

TABLE VI: Position state mapping used to construct the quantum circuit presented in Fig. 13. This mapping requires ancilla qubits to induce interference by merging equivalent multi-qubit states.

$\|x=0\rangle \equiv \|0000\rangle$
$\|x=1\rangle \equiv \{\|1000\rangle, \|0100\rangle, \|0010\rangle, \|0001\rangle\}$
$\|x=2\rangle \equiv \{\|1100\rangle, \|1010\rangle, \|1001\rangle, \|0110\rangle, \|0101\rangle, \|0011\rangle\}$
$\|x=3\rangle \equiv \{\|1110\rangle, \|1101\rangle, \|1011\rangle, \|0111\rangle\}$
$\|x=4\rangle \equiv \|1111\rangle$

TABLE VII: Output after each step of DQW and output of quantum circuit shown in Fig. 13 without the interference step provided by the ancilla circuit. Here $c_1, c_2, ...$ represents the contribution of cos(θ)-term from the coin operation in the first, second ... time-evolutions and similarly $s_1, s_2, ...$ represents the contribution of sin(θ)-term from the coin operation in the first, second ... time-evolutions, respectively in the circuit.

Steps	Directed quantum walk output	Circuit (Fig. 13) output without ancilla
0.	$\|0\rangle \otimes \|x=0\rangle$	$\|0\rangle \otimes \|0000\rangle$
1.	$c_1 \|0\rangle \otimes \|x=0\rangle + s_1 \|1\rangle \otimes \|x=1\rangle$	$c_1 \|0\rangle \otimes \|0000\rangle + s_1 \|1\rangle \otimes \|1000\rangle$
2.	$c_2c_1 \|0\rangle \otimes \|x=0\rangle + s_2c_1 \|1\rangle \otimes \|x=1\rangle + s_2s_1 \|0\rangle \otimes \|x=1\rangle - c_2s_1 \|1\rangle \otimes \|x=2\rangle$	$c_2c_1 \|0\rangle \otimes \|0000\rangle + s_2c_1 \|1\rangle \otimes \|0100\rangle + s_2s_1 \|0\rangle \otimes \|1000\rangle - c_2s_1 \|1\rangle \otimes \|1100\rangle$
3.	$c_3c_2c_1 \|0\rangle \otimes \|x=0\rangle + s_3c_2c_1 \|1\rangle \otimes \|x=1\rangle + s_3s_2c_1 \|0\rangle \otimes \|x=1\rangle - c_3s_2c_1 \|1\rangle \otimes \|x=2\rangle + c_3s_2s_1 \|0\rangle \otimes \|x=1\rangle + s_3s_2s_1 \|1\rangle \otimes \|x=2\rangle - s_3c_2s_1 \|0\rangle \otimes \|x=2\rangle + c_3c_2s_1 \|1\rangle \otimes \|x=3\rangle$	$c_3c_2c_1 \|0\rangle \otimes \|0000\rangle + s_3c_2c_1 \|1\rangle \otimes \|0010\rangle + s_3s_2c_1 \|0\rangle \otimes \|0100\rangle - c_3s_2c_1 \|1\rangle \otimes \|0110\rangle + c_3s_2s_1 \|0\rangle \otimes \|1000\rangle + s_3s_2s_1 \|1\rangle \otimes \|1010\rangle - s_3c_2s_1 \|0\rangle \otimes \|1100\rangle + c_3c_2s_1 \|1\rangle \otimes \|1110\rangle$
4.	$c_4c_3c_2c_1 \|0\rangle \otimes \|x=0\rangle + s_4c_3c_2c_1 \|1\rangle \otimes \|x=1\rangle + s_4s_3c_2c_1 \|0\rangle \otimes \|x=1\rangle - c_4s_3c_2c_1 \|1\rangle \otimes \|x=2\rangle + c_4s_3s_2c_1 \|0\rangle \otimes \|x=1\rangle + s_4s_3s_2c_1 \|1\rangle \otimes \|x=2\rangle - s_4c_3s_2c_1 \|0\rangle \otimes \|x=2\rangle + c_4c_3s_2c_1 \|1\rangle \otimes \|x=3\rangle + c_4c_3s_2s_1 \|0\rangle \otimes \|x=1\rangle + s_4c_3s_2s_1 \|1\rangle \otimes \|x=2\rangle + s_4s_3s_2s_1 \|0\rangle \otimes \|x=2\rangle - c_4s_3s_2s_1 \|1\rangle \otimes \|x=3\rangle - c_4s_3c_2s_1 \|0\rangle \otimes \|x=2\rangle - s_4s_3c_2s_1 \|1\rangle \otimes \|x=3\rangle + s_4c_3c_2s_1 \|0\rangle \otimes \|x=3\rangle - c_4c_3c_2s_1 \|1\rangle \otimes \|x=4\rangle$	$c_4c_3c_2c_1 \|0\rangle \otimes \|0000\rangle + s_4c_3c_2c_1 \|1\rangle \otimes \|0001\rangle + s_4s_3c_2c_1 \|0\rangle \otimes \|0010\rangle - c_4s_3c_2c_1 \|1\rangle \otimes \|0011\rangle + c_4s_3s_2c_1 \|0\rangle \otimes \|0100\rangle + s_4s_3s_2c_1 \|1\rangle \otimes \|0101\rangle - s_4c_3s_2c_1 \|0\rangle \otimes \|0110\rangle + c_4c_3s_2c_1 \|1\rangle \otimes \|0111\rangle + c_4c_3s_2s_1 \|0\rangle \otimes \|1000\rangle + s_4c_3s_2s_1 \|1\rangle \otimes \|1001\rangle + s_4s_3s_2s_1 \|0\rangle \otimes \|1010\rangle - c_4s_3s_2s_1 \|1\rangle \otimes \|1011\rangle - c_4s_3c_2s_1 \|0\rangle \otimes \|1100\rangle - s_4s_3c_2s_1 \|1\rangle \otimes \|1101\rangle + s_4c_3c_2s_1 \|0\rangle \otimes \|1110\rangle - c_4c_3c_2s_1 \|1\rangle \otimes \|1111\rangle$

TABLE VIII: Output after the three steps of a DQW using the quantum circuit shown in Fig. 13 and output of the quantum circuit with ancilla as shown in Fig. 14 after the interference step. Here $c_1, c_2, ...$ represents the contribution of $\cos(\theta)$-term from the coin operation in the first, second ... time-evolutions and similarly $s_1, s_2, ...$ represents the contribution of $\sin(\theta)$-term from the coin operation in the first, second ... time-evolutions, respectively in the circuit.

Step	Circuit output without ancilla	Circuit output with ancilla
3.	$\Big(c_3c_2c_1 \lvert 0\rangle \otimes \lvert 0000\rangle + s_3c_2c_1 \lvert 1\rangle \otimes \lvert 0010\rangle + s_3s_2c_1 \lvert 0\rangle \otimes \lvert 0100\rangle - c_3s_2c_1 \lvert 1\rangle \otimes \lvert 0110\rangle + c_3s_2s_1 \lvert 0\rangle \otimes \lvert 1000\rangle + s_3s_2s_1 \lvert 1\rangle \otimes \lvert 1010\rangle - s_3c_2s_1 \lvert 0\rangle \otimes \lvert 1100\rangle + c_3c_2s_1 \lvert 1\rangle \otimes \lvert 1110\rangle\Big) \otimes \lvert 0\rangle$	$\Big(c_3c_2c_1 \lvert 0\rangle \otimes \lvert 0000\rangle \otimes \lvert 0\rangle + s_3c_2c_1 \lvert 1\rangle \otimes \lvert 0010\rangle \otimes \lvert 0\rangle + s_3s_2c_1 \lvert 0\rangle \otimes \lvert 0100\rangle \otimes \lvert 0\rangle + c_3s_2s_1 \lvert 0\rangle \otimes \lvert 0100\rangle \otimes \lvert 1\rangle + s_3s_2s_1 \lvert 1\rangle \otimes \lvert 0110\rangle \otimes \lvert 1\rangle - c_3s_2c_1 \lvert 1\rangle \otimes \lvert 0110\rangle \otimes \lvert 0\rangle - s_3c_2s_1 \lvert 0\rangle \otimes \lvert 1100\rangle \otimes \lvert 1\rangle + c_3c_2s_1 \lvert 1\rangle \otimes \lvert 1110\rangle \otimes \lvert 1\rangle\Big)$

TABLE IX: Output after the four steps of a DQW using the quantum circuit shown in Fig. 13 and output of the quantum circuit with ancilla as shown in Fig. 15 after the interference step. Here $c_1, c_2, ...$ represents the contribution of $\cos(\theta)$-term from the coin operation in the first, second ... time-evolutions and similarly $s_1, s_2, ...$ represents the contribution of $\sin(\theta)$-term from the coin operation in the first, second ... time-evolutions, respectively in the circuit.

Step	Circuit output without ancilla	Circuit Output with ancilla
4.	$\Big(c_4c_3c_2c_1 \lvert 0\rangle \otimes \lvert 0000\rangle + s_4c_3c_2c_1 \lvert 1\rangle \otimes \lvert 0001\rangle + s_4s_3c_2c_1 \lvert 0\rangle \otimes \lvert 0010\rangle - c_4s_3c_2c_1 \lvert 1\rangle \otimes \lvert 0011\rangle + c_4s_3s_2c_1 \lvert 0\rangle \otimes \lvert 0100\rangle + s_4s_3s_2c_1 \lvert 1\rangle \otimes \lvert 0101\rangle - s_4c_3s_2c_1 \lvert 0\rangle \otimes \lvert 0110\rangle + c_4c_3s_2c_1 \lvert 1\rangle \otimes \lvert 0111\rangle + c_4c_3s_2s_1 \lvert 0\rangle \otimes \lvert 1000\rangle + s_4c_3s_2s_1 \lvert 1\rangle \otimes \lvert 1001\rangle + s_4s_3s_2s_1 \lvert 0\rangle \otimes \lvert 1010\rangle - c_4s_3s_2s_1 \lvert 1\rangle \otimes \lvert 1011\rangle - c_4s_3c_2s_1 \lvert 0\rangle \otimes \lvert 1100\rangle - s_4s_3c_2s_1 \lvert 1\rangle \otimes \lvert 1101\rangle + s_4c_3c_2s_1 \lvert 0\rangle \otimes \lvert 1110\rangle - c_4c_3c_2s_1 \lvert 1\rangle \otimes \lvert 1111\rangle\Big) \otimes \lvert 000\rangle$	$c_4c_3c_2c_1 \lvert 0\rangle \otimes \lvert 0000\rangle \otimes \lvert 000\rangle + s_4c_3c_2c_1 \lvert 1\rangle \otimes \lvert 0001\rangle \otimes \lvert 000\rangle + s_4s_3c_2c_1 \lvert 0\rangle \otimes \lvert 0100\rangle \otimes \lvert 001\rangle + c_4s_3s_2c_1 \lvert 0\rangle \otimes \lvert 0100\rangle \otimes \lvert 000\rangle + c_4c_3s_2s_1 \lvert 0\rangle \otimes \lvert 0100\rangle \otimes \lvert 100\rangle + s_4c_3s_2s_1 \lvert 1\rangle \otimes \lvert 0101\rangle \otimes \lvert 100\rangle - c_4s_3c_2c_1 \lvert 1\rangle \otimes \lvert 0101\rangle \otimes \lvert 001\rangle + s_4s_3s_2c_1 \lvert 1\rangle \otimes \lvert 0101\rangle \otimes \lvert 000\rangle + s_4s_3s_2s_1 \lvert 0\rangle \otimes \lvert 0110\rangle \otimes \lvert 101\rangle - s_4c_3s_2c_1 \lvert 0\rangle \otimes \lvert 0110\rangle \otimes \lvert 001\rangle - c_4s_3c_2s_1 \lvert 0\rangle \otimes \lvert 0110\rangle \otimes \lvert 010\rangle + c_4c_3s_2c_1 \lvert 1\rangle \otimes \lvert 0111\rangle \otimes \lvert 001\rangle - c_4s_3s_2s_1 \lvert 1\rangle \otimes \lvert 0111\rangle \otimes \lvert 101\rangle - s_4s_3c_2s_1 \lvert 1\rangle \otimes \lvert 0111\rangle \otimes \lvert 110\rangle + s_4c_3c_2s_1 \lvert 0\rangle \otimes \lvert 1110\rangle \otimes \lvert 111\rangle - c_4c_3c_2s_1 \lvert 1\rangle \otimes \lvert 1111\rangle \otimes \lvert 111\rangle$

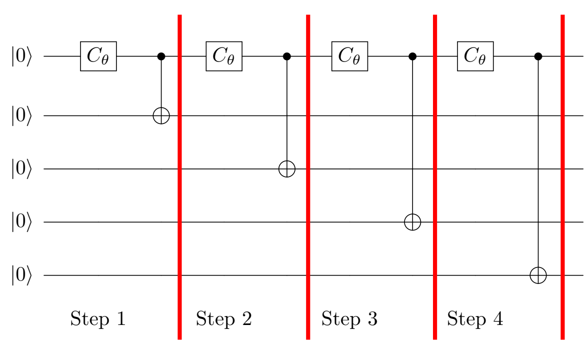

FIG. 13: Quantum circuit for DQW for first four steps without interference. Each step of this quantum circuit is given by a controlled-NOT gate because of the mapping chosen (see table VI). To include interference in the circuit, ancilla operations are needed before the measurement (see Fig. 15).

After the first three steps, a single ancilla qubit introduces the equivalence of the states with two qubits in state $|1\rangle$ to position space at $|x = 2\rangle$ as shown in Fig. 14. After the operation on ancilla qubit, the DQW distribution after 3 steps is recovered. Table VIII, shows the equivalence of the output of the third step of the DQW to the circuit output after the first three steps with an ancilla qubit operation before the Hadamard operation is performed on ancilla qubit. Similarly, to include interference after four steps, we need 3 ancilla qubits as shown in Fig. 15 and the

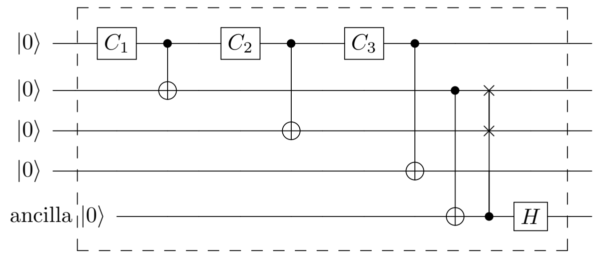

FIG. 14: Quantum circuit for DQW with the ancilla operation to include interference after first three steps. The ancilla qubit is left unobserved in the circuit. Here $C_1 = C_2 = C_3 = C_\theta$.

output equivalence is shown in table IX before the Hadamard gate is performed on the ancilla qubit. The Hadamard operation helps in un-entangling the ancilla qubit with the real qubits in the circuit.

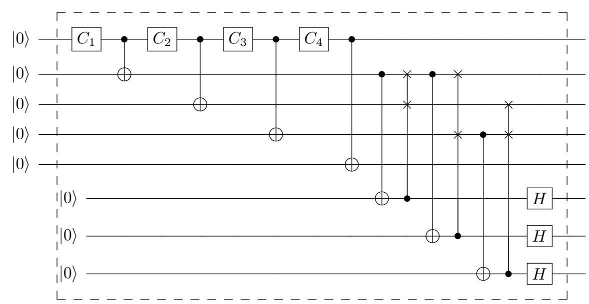

FIG. 15: Quantum circuit for DQW with ancilla operation to include interference after the first four steps. The ancilla qubits are left unobserved in the circuit. With a larger number of steps, the number of ancilla qubits also increases. Here $C_1 = C_2 = C_3 = C_4 = C_\theta$.

The number of ancilla qubits as well as Fredkin (CSWAP) gates for the circuit in Fig. 13 increases as ${}^{n-1}C_2$ where, n is the step number after which the measurement is done. The ancilla operation is needed only before the measurement.

From Fig. 15, it can be seen that for the first four steps of DQW, the number of CNOT-gate required is 7 along with 3 Fredkin- gates. Each Fredkin- gate can be decomposed into 5 two-qubit gate [76]. Therefore, total number of two-qubit gates required for first four steps of DQW using ancilla qubits are 22. Compared to this, if we look at the DQW circuit without ancilla, for the first four steps the number of CNOT gate required is 4, number of Toffoli gate is 3, and number of controlled-Toffoli (CCCNOT) gate is 2 as can be seen in Figs. 9 and 11. Each Toffoli gate can be decomposed into 6 CNOT-gates and each CCCNOT gate can be further decomposed into two qubit gate and Toffoli gates [77]. The number of two-qubit gates required for first four steps of DQW without use of ancilla qubits will be far more than the 22. Therefore, a processor with access to large number of qubits with an possibility to leave anclilla qubit unobserved [78, 79] can be effective in reducing the gate counts to implement DTQW.